Microfocusing transfocator for 1D and 2D compound refractive lenses

A. V. Zozulya,* S. Bondarenko, A. Schavkan, F. Westermeier, G. Grübel, and M. Sprung

Deutsches Elektronen-Synchrotron DESY, Notkestraße 85, D-22607 Hamburg, Germany
**alexey.zozulya@desy.de*

Abstract: An x-ray transfocator design for the combined use of 1D and 2D compound refractive lenses is described. The device includes stacks of beryllium parabolic lenses with different radii of curvature and provides microfocused x-ray beams in the 4-20 keV photon energy range. The transfocator has been implemented at the P10 Coherence Beamline of the PETRA III synchrotron at DESY, Hamburg. Results of transfocator performance and applications for coherent x-ray scattering experiments are presented.

OCIS codes: (340.7460) X-ray microscopy; (120.3620) Lens system design; (030.6140) Speckle; (100.5070) Phase retrieval; (160.5298) Photonic crystals.

References and links

1. B. Lengeler, C. Schroer, J. Tümmler, B. Benner, M. Richwin, A. Snigirev, I. Snigireva, and M. Drakopoulos, "Imaging by parabolic refractive lenses in the hard x-ray range," J. Synchrotron Radiat. **6**(6), 1153–1167 (1999).
2. B. Lengeler, C. G. Schroer, M. Kuhlmann, B. Benner, T. F. Günzler, O. Kurapova, F. Zontone, A. Snigirev, and I. Snigireva, "Refractive x-ray lenses," J. Phys. D Appl. Phys. **38**(10A), A218–A222 (2005).
3. Homepage of B. Lengeler group at RWTH Aachen, Germany, *http://www.physik.rwth-aachen.de/en/institutes/institute-iib/group-lengeler/*.
4. A. Snigirev, I. Snigireva, G. Vaughan, J. Wright, M. Rossat, A. Bytchkov, and C. Curfs, "High energy x-ray transfocator based on Al parabolic refractive lenses for focusing and collimation," J. Phys.: Conf. Ser. **186**, 012073 (2009).
5. G. B. M. Vaughan, J. P. Wright, A. Bytchkov, M. Rossat, H. Gleyzolle, I. Snigireva, and A. Snigirev, "X-ray transfocators: focusing devices based on compound refractive lenses," J. Synchrotron Radiat. **18**(2), 125–133 (2011).
6. T. Schubert, "Design of the CRL transfocators for P08 and P09," DESY internal report.
7. R. Döhrmann, S. Botta, G. Falkenberg, T. Schubert, S. V. Roth, "The compound refractive lens changer for PETRA III," Highlights and HASYLAB Annual Report, 98–99 (2009).
8. G. Grübel and F. Zontone, "Correlation spectroscopy with coherent x-rays," J. Alloy. Comp. **362**(1-2), 3–11 (2004).
9. M. Leitner, B. Sepiol, L.-M. Stadler, B. Pfau, and G. Vogl, "Atomic diffusion studied with coherent X-rays," Nat. Mater. **8**(9), 717–720 (2009).
10. A. Madsen, R. L. Leheny, H. Guo, M. Sprung, and O. Czakkel, "Beyond simple exponential correlation functions and equilibrium dynamics in x-ray photon correlation spectroscopy," New J. Phys. **12**(5), 055001 (2010).
11. I. Robinson, G. Grübel, and S. Mochrie, "X-ray beams with high coherence," New J. Phys. **12**(3), 035002 (2010).
12. D. Sayre, H. N. Chapman, and J. Miao, "On the extendibility of x-ray crystallography to noncrystals," Acta Crystallogr. A **54**(2), 232–239 (1998).
13. I. K. Robinson, I. A. Vartanyants, G. J. Williams, M. A. Pfeifer, and J. A. Pitney, "Reconstruction of the shapes of gold nanocrystals using coherent x-ray diffraction," Phys. Rev. Lett. **87**(19), 195505 (2001).
14. A. V. Zozulya, O. M. Yefanov, I. A. Vartanyants, K. Mundboth, C. Mocuta, T. H. Metzger, J. Stangl, G. Bauer, T. Boeck, and M. Schmidbauer, "Imaging of nanoislands in coherent grazing-incidence small-angle x-ray scattering experiments," Phys. Rev. B **78**(12), 121304 (2008).
15. E. Lima, L. Wiegart, P. Pernot, M. Howells, J. Timmins, F. Zontone, and A. Madsen, "Cryogenic x-ray diffraction microscopy for biological samples," Phys. Rev. Lett. **103**(19), 198102 (2009).
16. Technical Design Report of PETRA III, *http://petra3.desy.de/sites/site_petra3/content/general/tdr/index_eng.html*.

#170431 - $15.00 USD Received 12 Jun 2012; accepted 16 Jul 2012; published 2 Aug 2012

17. D. H. Bilderback, P. Elleaume, and E. Weckert, "Review of third and next generation synchrotron light sources," J. Phys. At. Mol. Opt. Phys. **38**(9), S773–S797 (2005).
18. H. Franz, O. Leupold, R. Röhlsberger, S. V. Roth, O. H. Seeck, J. Spengler, J. Strempfer, M. Tischer, J. Viefhaus, E. Weckert, and T. Wroblewski, "PETRA III: DESY's new high brilliance third generation synchrotron radiation source," Synchrotron Radiat. News **19**(6), 25–29 (2006).
19. D. L. Abernathy, G. Grübel, S. Brauer, I. McNulty, G. B. Stephenson, S. G. J. Mochrie, A. R. Sandy, N. Mulders, and M. Sutton, "Small-angle X-ray scattering using coherent undulator radiation at the ESRF," J. Synchrotron Radiat. **5**(1), 37–47 (1998).
20. O. K. S. Tsui, S. G. J. Mochrie, and L. E. Berman, "Statistical analysis of x-ray speckle at the NSLS," J. Synchrotron Radiat. **5**(1), 30–36 (1998).
21. L. Antl, J. W. Goodwin, R. D. Hill, R. H. Ottewill, S. M. Owens, S. Papworth, and J. A. Waters, "The preparation of poly(methyl methacrylate) latices in non-aqueous media," Colloids Surf. **17**(1), 67–78 (1986).
22. C. Pathmamanoharan, C. Slob, and H. N. W. Lekkerkerker, "Preparation of polymethylmethacrylate latices in non-polar media," Colloid Polym. Sci. **267**(5), 448–450 (1989).
23. Y. A. Vlasov, X.-Z. Bo, J. C. Sturm, and D. J. Norris, "On-chip natural assembly of silicon photonic bandgap crystals," Nature **414**(6861), 289–293 (2001).
24. P. Schall, I. Cohen, D. A. Weitz, and F. Spaepen, "Visualization of dislocation dynamics in colloidal crystals," Science **305**(5692), 1944–1948 (2004).
25. P. Jiang, J. F. Bertone, K. S. Hwang, and V. L. Colvin, "Single-crystal colloidal multilayers of controlled thickness," Chem. Mater. **11**(8), 2132–2140 (1999).
26. J. Hilhorst, V. V. Abramova, A. Sinitskii, N. A. Sapoletova, K. S. Napolskii, A. A. Eliseev, D. V. Byelov, N. A. Grigoryeva, A. V. Vasilieva, W. G. Bouwman, K. Kvashnina, A. Snigirev, S. V. Grigoriev, and A. V. Petukhov, "Double stacking faults in convectively assembled crystals of colloidal spheres," Langmuir **25**(17), 10408–10412 (2009).
27. J. R. Fienup, "Phase retrieval algorithms: a comparison," Appl. Opt. **21**(15), 2758–2769 (1982).
28. A. V. Petukhov, J. H. J. Thijssen, D. C. Hart, A. Imhof, A. van Blaaderen, I. P. Dolbnya, A. Snigirev, A. Moussaid, and I. Snigireva, "Microradian x-ray diffraction in colloidal photonic crystals," J. Appl. Cryst. **39**(2), 137–144 (2006).
29. J. Gulden, O. M. Yefanov, A. P. Mancuso, V. V. Abramova, J. Hilhorst, D. Byelov, I. Snigireva, A. Snigirev, A. V. Petukhov, and I. A. Vartanyants, "Coherent x-ray imaging of defects in colloidal crystals," Phys. Rev. B **81**(22), 224105 (2010).

1. Introduction

X-ray focusing devices have become standard components at beamlines of modern synchrotrons. Focusing optics provides an x-ray probe with a size ranging from tens of microns down to tens of nanometers and a thousand-fold gain of photon flux density. There exist different designs of x-ray focusing optics based on curved mirrors, multilayers, bent crystals, capillary optics, Fresnel zone plates and compound refractive lenses. Among the above mentioned optics the x-ray focusing systems based on compound refractive lenses (CRLs) represent certain advantages, namely, on-axis geometry, absence of spherical aberrations, suitability for hard x-ray energy range, simplicity of alignment and radiation hardness [1, 2]. The fabrication technique of parabolic refractive lenses has made significant progress [3]. The high-quality beryllium refractive lenses are commercially available and can serve as building blocks of on-axis focusing devices for hard x-ray beamlines at 3rd generation synchrotrons and free-electron laser facilities.

Refractive x-ray lenses are strongly chromatic optical elements with a focal distance being proportional to the photon energy squared. Thus, a number of individual lenses has to be grouped together to produce a focused beam for the required photon energy and the focal distance. Over the last years *transfocator* designs based on movable stacks of 2D CRLs have been proposed [4–7]. In this article the next generation of a CRL transfocator is presented. The new transfocator design combines the standard 2D lenses and the newly developed 1D beryllium lenses. This enables independent control over the focused beam size and shape in both transverse directions.

#170431 - $15.00 USD Received 12 Jun 2012; accepted 16 Jul 2012; published 2 Aug 2012

2. Experimental

2.1 P10 beamline

The Coherence Beamline P10 of the new storage ring PETRA III at DESY, Hamburg is dedicated to perform coherent x-ray scattering experiments using x-ray photon correlation spectroscopy (XPCS) and coherent diffraction imaging (CDI). XPCS is an x-ray technique analogous to dynamic light scattering in visible light range and based on the use of coherent x-rays to probe the dynamics of condensed matter by analyzing temporal correlations of coherent scattering patterns (or 'speckles') [8–11]. CDI is a high resolution imaging method aimed at 2D and 3D reconstruction of density distribution inside individual nanostructures or biological specimens [12–15]. Computational phase retrieval algorithms are used in this technique for *ab initio* image reconstruction from coherent x-ray diffraction patterns measured in a far field.

An ultimate aim of the P10 beamline is to employ the full coherent flux of an undulator source for coherent scattering experiments. The beamline is equipped with a 5 m-long undulator U29 located in a low-beta section of the PETRA III storage ring. The x-ray source has a vertical size of 14 μm and a horizontal size of 85 μm at full-width at half maximum (FWHM). These remarkably small values are achieved thanks to the unique design of the low-emittance storage ring PETRA III having 2304 m circumference [16–18]. Nevertheless, the horizontal source size is six times larger than the vertical size which results in the inverse asymmetry of transverse coherence lengths. Matching vertical and horizontal coherence lengths can provide a several-fold enhancement of the coherent photon flux at a sample. It is for this purpose the new transfocator design includes both 1D and 2D lenses. It is planned to implement an additional vertically prefocusing CRL transfocator, located far upstream from the end-station, which will create a secondary source at an intermediate distance along the optical path. The combined use of 1D and 2D CRLs will produce an image of a secondary source in vertical direction and an image of a primary source in horizontal direction at the same focal plane.

The x-ray optical scheme of the P10 beamline consists of a vertical double-crystal Si(111) monochromator and a pair of horizontally reflecting flat mirrors (Si, Rh and Pt stripes) for suppression of higher harmonics of an undulator spectrum. Owing to an extreme brilliance of the PETRA III source, the beamline provides highly intense monochromatic x-ray beam with a coherent photon flux above 10^{11} photons s^{-1} at the photon energy of 8 keV.

2.2 Transfocator design

The new design of a CRL transfocator is based on 1D and 2D beryllium parabolic refractive lenses manufactured at the RWTH Aachen [3]. The 2D lenses have rotationally parabolic shape and different radii of curvature ranging from 50 to 1500 μm. The actual 2D lens is mounted inside a high precision disk frame of 12 mm diameter (Fig. 1(a)) such that the centers of a lens and a disk match within a few microns. The 1D lens has a cylinder parabolic shape and its design is quite different. The lens is mounted in the center of a high precision square frame (20×20 mm^2) with the cylinder axis being parallel to the edge of a square (Fig. 1(b)). The 1D beryllium lenses are available with radii of curvature of 500, 1000 and 1500 μm.

The optical design of the transfocator represents a system of 12 lens stacks containing different number of 1D and 2D individual refractive lenses. Each lens stack contains a number of individual lenses N with a curvature radius R as listed in Table 1. The first 4 stacks (numeration starts from the stack facing a beam first) contain 1D lenses, and the next 8 stacks contain 2D lenses. Due to different frame shapes for 1D and 2D case, the 2D lenses are grouped in a cylindrical cartridge, while the 1D lenses are stacked inside a rectangular cartridge (Fig. 1(c, d)). Lens cartridges are aligned with respect to each other on a single 90 degree precision rail guide made of stainless steel (SKF, Germany). Each cartridge is attached

#170431 - $15.00 USD Received 12 Jun 2012; accepted 16 Jul 2012; published 2 Aug 2012

by a tension spring to an aluminum frame which is mechanically connected to a compact linear translation stage. Linear stages are driven by vacuum compatible linear piezo motors (PiezoMotor, Sweden) and equipped with end switches ensuring in and out of the beam positions for each CRL stack. The lens assembly is mounted inside an ultra-high vacuum (UHV) chamber such that the transfocator optics is operated in-vacuum. The UHV chamber is mounted on a positioning tower equipped with horizontal Y-translation (perpendicular to the beam), vertical Z-translation, and the corresponding two tilt stages, R_y and R_z (Huber, Germany). Underneath the positioning tower there is an X-translation stage (THK, Japan) providing ± 150 mm travel range along the beam and enabling a precise adjustment of a focal distance. The total transfocator length is 0.7 m (including the X-translation stage) which represents a relatively compact optical device which can be installed at different locations along the beamline path. In the present configuration the CRL transfocator is mounted on a granite table at the second experimental hutch of the P10 beamline at a distance of 85.5 m from a source. For the actual distance from the zero position of a transfocator to a sample position of 2.2 m the full 4-20 keV photon energy range can be explored. The mechanical design drawing and a photograph of the CRL transfocator installed at the beamline are shown in Fig. 2.

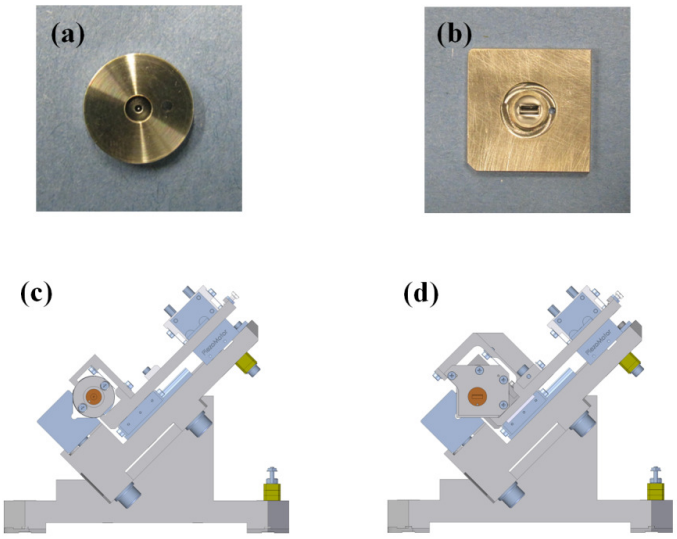

Fig. 1. Photographs of beryllium refractive lenses: (a) 2D rotationally parabolic lens and (b) 1D cylinder parabolic lens. Design drawings showing (c) the 2D lens stack holder and (d) the 1D lens stack holder (view along an optical axis).

Table 1. Arrangement of individual lenses of the transfocator

Stack	1	2	3	4	5	6	7	8	9	10	11	12
CRL type	1D	1D	1D	1D	2D	2D	2D	2D	2D	2D	2D	2D
N	1	2	4	8	1	1	1	2	1	2	4	8
R, µm	500	500	500	500	1000	500	200	200	50	50	50	50

#170431 - $15.00 USD Received 12 Jun 2012; accepted 16 Jul 2012; published 2 Aug 2012

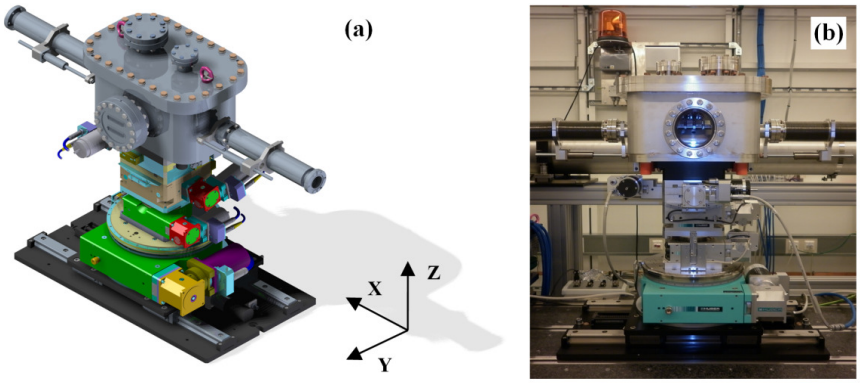

Fig. 2. (a) Design drawing of the CRL transfocator mounted on a 5-axis positioning stage. (b) Photograph of the transfocator installed at the P10 beamline.

3. Transfocator performance

3.1 Alignment

The transfocator contains 12 independent CRL stacks which results in 2^{12} = 4096 possible lens combinations. Each CRL combination can be represented by the 12-digit binary number or the corresponding decimal number *M*. In order to find the optimal combination for a given photon energy and an image distance one has to sort through all combinations and select the best one in terms of efficiency, gain, and number of lenses. Based on formulae given in [1] a Matlab script has been written to find the best lens combination and corresponding optical parameters such as actual focal distance, offset distance along an optical axis, transmittance, gain, focal spot size and depth of focus. Each stack of lenses is treated as one single lens consisting of *N* individual elements while the resulting optical parameters are calculated iteratively taking into account the actual device geometry.

Once the proper lens combination is defined, the transfocator has to be aligned in the beam. First, the transfocator position along an optical axis should match the focal length of a selected CRL at a given photon energy. This is done using the X-translation of the transfocator which moves the device from a zero position to an offset position ΔX. In a second step the optical axis of a device has to be aligned parallel to the beam direction, which is performed by Y-, Z- translations and R_y-, R_z- tilts. The fine tuning of the offset position can be performed by direct measurement of the beam size at a sample position as a function of an offset distance as shown in Fig. 3. The focal spot size (FWHM) has been measured as a function of the transfocator offset ΔX by scanning a Pt/Ir knife edge and registering the transmitted intensity on a calibrated Si diode. The CRL consisting of one stack of 8 lenses with R = 50 μm (*M* = 2048) has been used at a photon energy of 15 keV. The calculated offset for this case is 47 mm which corresponds to a minimum of the curve measured for the vertical spot size. For the horizontal focus position, we observed that it is offset by 17 mm relative to the vertical focus position towards larger focal distances. The observed astigmatism effect is apparently attributed to the horizontally reflecting mirror pair which defocuses the beam slightly and thereby creates a virtual source located at a closer distance to the sample than the actual source position.

An important parameter of the focusing device is the transmission (or efficiency) being a ratio of the intensity incident on an entrance aperture to the transmitted intensity. Transmission of different 1D (M = 8, 15) and 2D (M = 16, …, 2048) CRL combinations has been measured using a Si diode placed behind the transfocator. The results of measurements performed at the photon energy of 7.9 keV and the CRL illumination slit size of 200 × 200 μm^2 are given in Table 2 and show an excellent agreement with calculations.

#170431 - $15.00 USD Received 12 Jun 2012; accepted 16 Jul 2012; published 2 Aug 2012

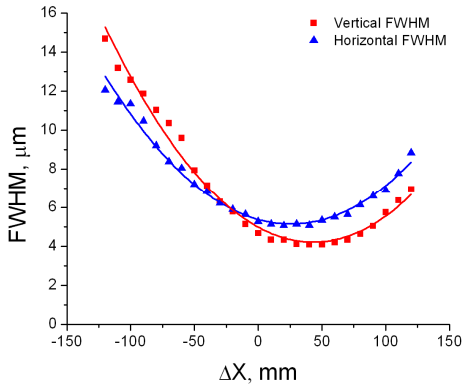

Fig. 3. Vertical (squares) and horizontal (triangles) focal spot sizes measured as a function of an offset ΔX. Solid lines represent parabolic fitting curves.

Table 2. Measured (T_{exp}) and calculated (T_{calc}) transmission for different CRL combinations

M	8	15	16	32	64	128	256	512	576	1024	1536	1792	2048
T_{exp}, %	86.6	76.0	98.6	97.9	96.7	92.6	89.7	83.8	81.8	69.6	60.0	52.5	50.3
T_{calc}, %	86.8	76.8	99.0	98.6	97.4	94.9	92.1	85.0	82.8	72.8	61.9	57.0	54.7

3.2 Focal spot measurement

The main function of the described transfocator is to focus an x-ray beam on a sample placed at a certain distance downstream of the device. In order to determine the size of a focal spot produced by the CRL transfocator we used conventional knife edge scanning across the focal spot. The beam was focused onto the slit aperture located at 1.91 m distance downstream the transfocator, and one of the polished Ta slit blades has been used for knife edge scanning in vertical and horizontal directions. The transmitted intensity was detected by avalanche photodiode placed behind the knife edge. No additional apertures were introduced between lens and knife edge. For the selected photon energy of E = 13.2 keV the CRL consisting of 7 lenses with R = 50 μm (M = 1792, stack numbers 9, 10, 11) has been employed.

In the experiment, a special attention has been paid to the selection of the size of a CRL entrance aperture which was defined by the G2 in-vacuum slit located 1.5 m upstream the transfocator. Different slit settings have been applied and the optimum size of 100 × 100 μm^2 (providing the smallest focal spot) has been selected. For vertical direction the demagnified source size is 0.4 μm which is about five times smaller than the broadening of a focal spot due to Fraunhofer diffraction on the entrance aperture. Oppositely, for horizontal direction the spot size is mainly defined by the demagnified image of a source. Under these experimental conditions the focal spot sizes of 2.9(h) × 2.9(v) μm^2 have been measured showing a good agreement with the calculated values of 2.8(h) × 2.2(v) μm^2 (Fig. 4). Noticeably, for the horizontal direction a very good match between experimental and theoretical values is achieved. In the vertical direction the experimental spot size exceeds the calculated value by ~30% which can be attributed to vertical disturbances of the cryo-cooled monochromator optics.

#170431 - $15.00 USD Received 12 Jun 2012; accepted 16 Jul 2012; published 2 Aug 2012

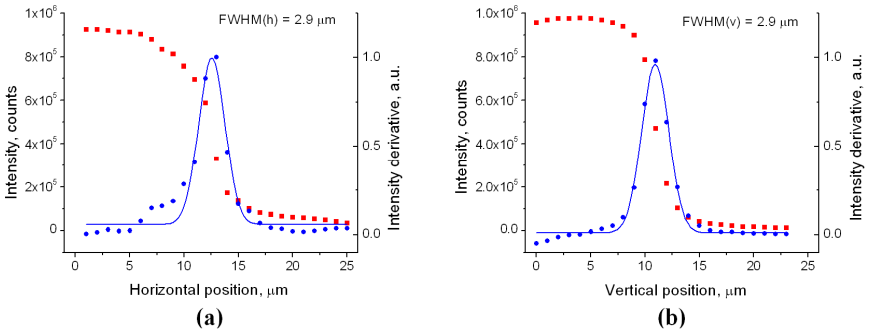

Fig. 4. Focal spot sizes measured (a) in horizontal and (b) in vertical directions by knife edge scanning. Experimental data are represented by red squares, derivative curves and gaussian fits are shown by blue cycles and blue solid lines respectively.

3.3 Intensity contrast measurement

The influence of an entrance aperture of a CRL on the speckle contrast is of large importance for coherent scattering experiments utilizing focused beams. In other words, the lens illumination slit has to be adjusted to an optimal size in order to provide a maximum flux of coherent x-ray photons and maintain a high contrast at the same time. These settings can vary depending on optical design and geometrical parameters of a particular instrument. For this purpose the measurements of static speckles [19, 20] from dried colloidal systems have been performed at P10 using the microfocused beam delivered by the CRL transfocator. The speckle contrast values have been evaluated as a function of the lens illumination aperture size.

Colloidal systems consisting of polymethylmethacrylate (PMMA) particles dispersed in decalin have been used in the experiment. The samples were synthesized as described in references [21, 22]. The colloidal sample was filled into a quartz capillary of 1 mm diameter and dried in vacuum. The particle radius of 126 nm and a polydispersity of about 7% were determined from the formfactor of diluted sample. Speckle images were collected at a photon energy of 8 keV using the pixelated 2D detector MAXIPIX (516 × 516 px^2 active area, 55.5 μm pixel size, 1 ms readout time). The CRL combination consisting of a single lens of 200 μm radius and 2 lenses of 50 μm radius (M = 576, stack numbers 7 and 10) was used to focus x-ray beam onto a sample located 2.16 m downstream the transfocator. The CRL illumination slit G2 was set to constant horizontal sizes of 50, 75 and 100 μm while the vertical opening was varied from 50 to 300 μm. To assure the same average level of scattering intensity over all measured data sets the speckles were acquired by recording 20 detector frames with exposure times varied in 0.25 - 4.5 s range depending on slit settings.

Scattering contrast β of measured speckles has been analyzed using the Matlab-based software package XPCS GUI (developed at the APS). Using the XPCS GUI each scattering pattern was binned into 20 radial partitions representing concentric rings around the beam center. For each partition the speckle contrast has been calculated as $\beta = \sigma(I)^2/\langle I\rangle^2$, where $\sigma(I)$ and $\langle I\rangle$ are the standard deviation and the mean intensity per pixel over the selected partition area. Figure 5 displays the speckle contrast curves measured as a function of the vertical size of G2 slit and obtained for a range of scattering vectors 0.0054 - 0.0058 $Å^{-1}$. Contrast values above 50% have been observed in this experiment indicating a high degree of transverse coherence of a focused beam.

#170431 - $15.00 USD Received 12 Jun 2012; accepted 16 Jul 2012; published 2 Aug 2012

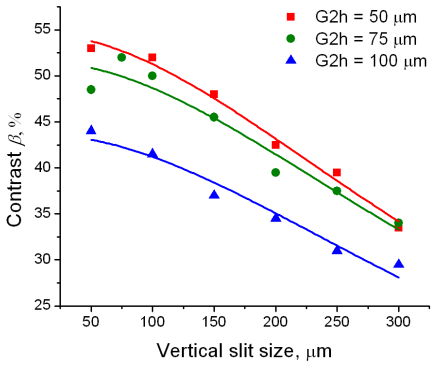

Fig. 5. Speckle contrast β measured as a function of the vertical size of CRL entrance slit G2 at the constant horizontal sizes of 50, 75 and 100 μm. Solid lines represent the fitting curves.

The scattering contrast can be expressed via a detector pixel size p and a minimum 'speckle' size S_{min}:

$$\beta = B / \left(1 + \left(p / S_{\min}\right)^2\right), \tag{1}$$

where B is a fitting coefficient describing a maximum contrast value which could be achieved using a detector with an infinitely small pixel size. The minimum 'speckle' size is the smallest scattering feature defined by the beam size D as $S_{min} = \lambda L_{sd} / D$, where L_{sd} is the sample-to-detector distance and λ is the x-ray wavelength. The size D of a focused beam at a sample was taken as

$$D = 1.22\lambda L_q / d_{sl} + C d_{sl}. \tag{2}$$

Here d_{sl} is the size of the CRL entrance slit, L_q is the lens-to-sample distance, and C is a fitting parameter. The term representing a demagnified source size is omitted in (2) as it is small compared to the diffraction term. The presence of a term proportional to the slit size is related to the forward scattering fraction of the incident beam (Compton scattering from lens material [1, 2]) and results in the contrast decrease for larger illumination slit sizes. The reduction of the transverse coherence of a focused beam caused by forward scattering background implies a certain limit on the size of the CRL illumination slit for coherent scattering experiments. As follows from our analysis this size is several times smaller than the effective aperture of the CRL (~500 μm).

Experimental contrast curves have been fitted using Eq. (1) and Eq. (2), and the results are summarized in Table 3, where *G2h* denotes the horizontal size of CRL entrance slit G2 and β_{max} is the maximum contrast measured at a given horizontal slit setting. Obtained contrast curves show that for vertical slit sizes larger than 150 μm the contrast starts to decrease by more than 20% as compared to the maximum value. It is also observed that the contrast values measured for *G2h* slit size of 100 μm are ~20% lower than the contrast level obtained for 50 μm and 75 μm slit settings. From the analysis of contrast curves we conclude that for the used photon energy of 8 keV a reasonable compromise between coherent photon flux and scattering contrast can be achieved with a CRL entrance slit size of 75(h) × 150(v) μm^2.

Table 3. Contrast values and fitting results

G2h, μm	β_{max}, %	*B*, %	*C*	χ^2
50	53.8	54.8	0.036	0.99
75	51.2	53.3	0.037	0.96
100	43.1	43.9	0.035	0.96

#170431 - $15.00 USD Received 12 Jun 2012; accepted 16 Jul 2012; published 2 Aug 2012

4. CDI application

High degree of transverse coherence of the x-ray beam is a prerequisite for coherent x-ray diffraction experiments. Finite detector resolution (pixel size) poses certain constraints on the size of the beam illuminating a sample, namely, the minimum speckle size has to be larger than the pixel size of a detector. For the experiment, this means that the beam size at the sample has to be limited to a size of several tens of microns resulting in dramatic reduction of incident photon flux. Exploiting x-ray focusing it is possible to confine the beam without a loss of photon flux.

Aiming to reveal the local structure of a hard-sphere colloidal crystal we have performed the CDI experiment using a coherently focused beam produced by the CRL transfocator. The colloidal crystals have shown promising applications as photonic crystals [23] although a high concentration of misfit dislocations hampers their implementation in real photonic devices [24]. We have studied a thin crystalline film of self-assembled polystyrene microspheres of 162 nm diameter. The crystal was grown by the vertical deposition technique on a glass substrate [25, 26]. Measurements were carried out in transmission geometry at a photon energy of 15 keV. X-ray beam was focused using the CRL combination of 8 lenses with 50 μm curvature radius (M = 2048, stack number 12) and the lens illumination slit size of 100 × 100 μm^2. Coherent x-ray diffraction patterns have been acquired using the MAXIPIX pixel detector (see §4 for the detector parameters) positioned at a distance of 5.2 m behind a sample. The sample-to-detector distance and the pixel size of a detector define the achieved resolution in reciprocal space of 8.1×10^{-5} Å^{-1}, which, being multiplied by a detector image size, gives the maximum range of measured scattering vectors of 4.2×10^{-2} Å^{-1}. The MAXIPIX detector allows for fast series of images to be recorded, and typically 100 frames with exposure times of 0.1 s per frame have been collected. The direct transmitted x-ray beam was blocked by a beamstop of 3 mm diameter which was placed inside the evacuated flight tube.

The coherent x-ray diffraction pattern measured from the high-quality domain of a colloidal crystal is shown in Fig. 6(a). Bragg diffraction peaks up to (440) reflection and intensity oscillations due to the form factor of a colloidal sphere up to 7th order are clearly observed in the diffraction pattern. Experimental data have been processed using iterative phase retrieval approach. This technique is based on computational inversion of diffraction pattern in order to obtain a real space image by alternately applying direct and inverse 2D Fourier transform operations. The measured intensities provide input scattering amplitudes for the reconstruction procedure while unknown phases are iteratively refined by the algorithm. The maximum range of measured scattering vectors defines the pixel size of 15 nm in the reconstructed image. Experimental data were masked to eliminate inactive pixels and corrected for a flatfield response of the detector. Prior to starting a reconstruction procedure the CDI pattern was binned to 258 × 258 px^2 size. For phase retrieval reconstruction we have applied the hybrid input-output (HIO) algorithm [27] with a circular support of 30 px radius. The central region of 100 × 100 px^2 of the reconstruction image is presented in Fig. 6(b). The resulting image was obtained by an average over 70 independent reconstruction runs started from a random set of phases. The transverse profile of a focused beam has been taken into account by normalizing the obtained image by a broad gaussian distribution of 36 px width. In the reconstructed image one can clearly observe the projected density of colloidal spherical particles arranged in hexagonal close-packed structure [28, 29]. From the reconstruction result, the distance a = 96 nm between adjacent maxima has been determined which corresponds to the actual interparticle distance (sphere diameter) of $d = a\sqrt{3}$ = 166 nm. The reconstructed diameter of colloidal microspheres agrees well with the nominal particle size of 162 nm obtained from the crystal manufacturer.

#170431 - $15.00 USD Received 12 Jun 2012; accepted 16 Jul 2012; published 2 Aug 2012

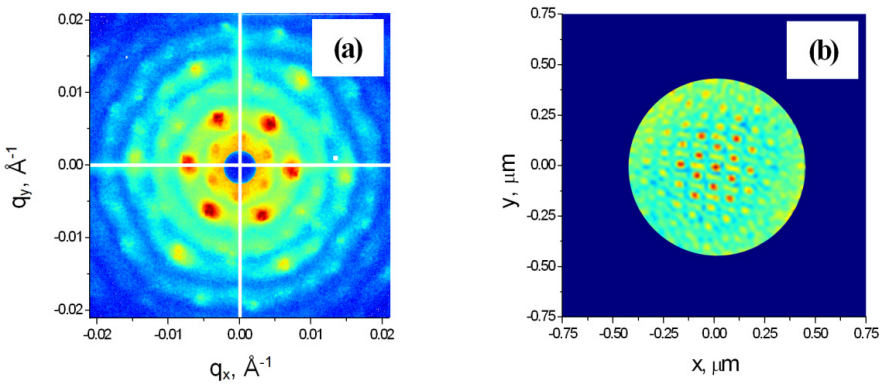

Fig. 6. (a) Coherent diffraction pattern measured from a colloidal crystal using CRL focused x-rays. Intensity values are logarithmically scaled. (b) Reconstructed image of the illuminated sample area.

5. Summary

The new x-ray transfocator featuring 1D and 2D parabolic refractive lenses has been designed and implemented at the P10 Coherence Beamline of the PETRA III synchrotron at DESY, Hamburg. Using different lens combinations it is possible to obtain a microfocused x-ray beam in the photon energy range between 4 and 20 keV. Results of transfocator testing confirm the straightforward alignment and the stable performance of the device. The focal spot sizes of less than 3 × 3 μm^2 have been measured by knife edge scanning at a photon energy of 13.2 keV and the actual distance between transfocator and knife edge of 1.91 m.

In order to find optimal conditions in terms of spatial coherence and coherent photon flux of a CRL focused beam, the static speckles from dried colloidal particles have been measured as a function of the CRL entrance aperture size. Statistical analysis of speckles measured at 8 keV photon energy has revealed contrast values above 50% and an optimal illumination slit size of 75(h) × 150(v) μm^2 has been established.

Coherent microfocused x-ray beam produced by the CRL transfocator at the P10 beamline has been employed for coherent diffraction imaging of a colloidal crystal made of polystyrene microspheres. The coherent diffraction patterns measured from a colloidal crystal film in transmission at a photon energy of 15 keV have been reconstructed to yield the direct image of projected density of close-packed spherical particles. The reconstructed diameter of colloidal microspheres is in a good agreement with the particle size provided by the crystal manufacturer.

The obtained results demonstrate that the new transfocator performs as predicted. Focal spot sizes of less than 5 μm in both transverse directions are routinely achieved and the spatial coherence is preserved in a focused x-ray beam under coherent illumination conditions.

Acknowledgments

Authors would like to thank B. Fischer for preparing the dried colloidal sample, D. Byelov, J.-M. Meijer and A.V. Petukhov for providing the colloidal crystal film and G. Falkenberg for a careful reading of the manuscript and valuable remarks.

#170431 - $15.00 USD Received 12 Jun 2012; accepted 16 Jul 2012; published 2 Aug 2012